Uterine histopathology and steroid metabolism in a polycystic ovary syndrome rat model

Gisela Soledad Bracho, María Virginia Acosta, Gabriela Anahí Altamirano, Mirta Raquel Alcaraz, Milagros Montemurro, María Julia Culzoni, María Florencia Rossetti, Laura Kass, Enrique Hugo Luque, Verónica Lis Bosquiazzo

PII: S0303-7207(24)00054-6

DOI: https://doi.org/10.1016/j.mce.2024.112198

Reference: MCE 112198

To appear in: *Molecular and Cellular Endocrinology*

Received Date: 26 December 2023

Revised Date: 23 February 2024

Accepted Date: 4 March 2024

Please cite this article as: Bracho, G.S., Acosta, Marí.Virginia., Altamirano, Gabriela.Anahí., Alcaraz, M.R., Montemurro, M., Culzoni, Marí.Julia., Rossetti, Marí.Florencia., Kass, L., Luque, E.H., Bosquiazzo, Veró.Lis., Uterine histopathology and steroid metabolism in a polycystic ovary syndrome rat model, *Molecular and Cellular Endocrinology* (2024), doi: https://doi.org/10.1016/j.mce.2024.112198.

TITLE: UTERINE HISTOPATHOLOGY AND STEROID METABOLISM IN A POLYCYSTIC OVARY SYNDROME RAT MODEL

AUTHORS: Gisela Soledad Bracho*[a,b], María Virginia Acosta*[a], Gabriela Anahí Altamirano[a,c], Mirta Raquel Alcaraz[e], Milagros Montemurro[e], María Julia Culzoni[e], María Florencia Rossetti[a,d], Laura Kass[a,c], Enrique Hugo Luque[a], Verónica Lis Bosquiazzo [a,d] #

[a] Instituto de Salud y Ambiente del Litoral (ISAL, UNL-CONICET), Facultad de Bioquímica y Ciencias Biológicas, Universidad Nacional del Litoral, Santa Fe, Argentina

[b] Departamento de Química General e Inorgánica. Facultad de Bioquímica y Ciencias Biológicas, Universidad Nacional del Litoral, Santa Fe, Argentina

[c] Cátedra de Patología Humana, Facultad de Bioquímica y Ciencias Biológicas, Universidad Nacional del Litoral, Santa Fe, Argentina

[d] Departamento de Bioquímica Clínica y Cuantitativa, Facultad de Bioquímica y Ciencias Biológicas, Universidad Nacional del Litoral, Santa Fe, Argentina

[e] Laboratorio de Desarrollo Analítico y Quimiometría (LADAQ), Cátedra de Química Analítica I, Facultad de Bioquímica y Ciencias Biológicas, Universidad Nacional del Litoral, Santa Fe, Argentina.

This work was supported by grants from Agencia Nacional de Promoción Científica y Tecnológica (ANPCyT), Consejo Nacional de Investigaciones Científicas y Técnicas (CONICET) and Universidad Nacional del Litoral (UNL), Argentina.

*These authors contributed equally to this work.

ABBREVIATIONS: AR, androgen receptor; CT, cycle threshold; Cyp19a1, aromatase mRNA; E2, 17β-estradiol; ESR1, estrogen receptor alpha; ESR2, estrogen receptor beta; HOXA10, homeobox A10; Hsd17b2, hydroxysteroid 17-beta dehydrogenase 2 mRNA; PTEN, phosphatidylinositol -3,4,5-trisphosphate 3- phosphatase; Srd5a1, steroid 5 alpha-reductase 1 mRNA; Star, Steroidogenic Acute Regulatory mRNA; WNT5a, wingless-related MMTV integration site member 5a mRNA.

CORRESPONDING AUTHOR: Instituto de Salud y Ambiente del Litoral (ISAL, UNL-CONICET), Facultad de Bioquímica y Ciencias Biológicas, Universidad Nacional del Litoral, Ciudad Universitaria, Paraje El Pozo, Casilla de Correo 242, (3000) Santa Fe, Argentina. TEL/FAX: 54 342 4575207. E-MAIL: vlbosqui@fbcb.unl.edu.ar (V.L. Bosquiazzo).

ABSTRACT

The aim of this study was to investigate uterine lesions, uterine endocrine status and expression of genes involved in uterine differentiation in a rat model of polycystic ovary syndrome (PCOS). The possible involvement of the androgen receptor (AR) was also investigated. PCOS rats showed an increased incidence of uterine epithelial and glandular lesions and elevated serum testosterone level, which was not detected in uterine tissue. Uterine 17β-estradiol, estrone and progesterone were detected in 100%, 75% and 50% of the animals, respectively. This was associated with a decrease in *Star* and an increase in *Hsd17b2*, *Srd5a1* and *Cyp19a1*, suggesting that uterine steroids are not synthesized *de novo* in PCOS and that alterations in these enzymes may explain the absence of testosterone and low progesterone. In addition, ESR2 decreased and AR increased, suggesting possible steroid receptor crosstalk. Genes associated with uterine differentiation, PTEN and WNT5a, also showed reduced expression. PCOS rats treated with flutamide, an AR antagonist, were similar to PCOS rats in terms of uterine lesions, serum steroid levels, ESR2, PTEN and WNT5a expression. However, testosterone, AR and aromatase levels were similar to control rats, with decreased expression of ESR1 and HOXA10, suggesting that these expressions are AR dependent. Our results suggest that the primary cause of the observed uterine lesions in the PCOS rat model is the altered endocrine status and consequently changes in genes related to uterine differentiation.

KEYWORDS: polycystic ovary syndrome, steroidogenesis, steroidogenic enzymes, steroid receptors, uterine morphology.

1. INTRODUCTION

Polycystic ovary syndrome (PCOS) is one of the most common endocrine disorders, affecting 7-12 % of women of reproductive age (Skiba et al, 2018). The diagnostic criteria for PCOS are oligo- or anovulation, clinical and/or biochemical signs of hyperandrogenism and polycystic ovaries (Rotterdam ESHRE/ASRM-Sponsored PCOS Consensus Workshop Group, 2004). Clinical observations suggest that, in women with PCOS, hormone abnormalities lead to an increased risk of endometrial hyperplasia and carcinoma, and pregnancy complications (Barry et al, 2014; Yu et al, 2016). Moreover, in women with PCOS, the incidence of endometrial hyperplasia is higher than 35% (Cheung, 2001) and the risk of endometrial cancer is three times higher (Haoula et al, 2012). In obese women, this risk is also three-fold higher, important data considering that obesity is a predominant feature in PCOS (Shafiee et al, 2014). However, the reason why women with PCOS have higher the risk of developing uterine abnormalities is not yet completely understood.

In PCOS women, androgen excess is a common finding (Dumesic & Lobo, 2013). This excess (also called hyperandrogenemia) can increases estrogen levels by its peripheral conversion, leading to a higher exposure of the endometrium to estrogen (Hosseinzadeh et al, 2021). However, some women with PCOS showed 17β-estradiol (E2) level similar to those of healthy women (Codner et al, 2007). It has been described that exposure to high or chronic levels of estrogens results in development of endometrial cancer (Kaaks et al, 2002; Zukerberg et al, 2004). Most endometrial cancers occur due to an unopposed estrogen environment (Nees et al, 2022). In PCOS, estrogen stimulation is not sufficiently counterbalanced by progesterone (P4) due to anovulation or oligo-ovulation (Shang et al, 2012; Dumesic & Lobo, 2013). On the other hand, the target tissue response to hormones

also depends on their *in-situ* availability, which is partly regulated by the activity of tissue steroidogenic enzymes. Several studies have demonstrated that the activity of enzymes related to steroid metabolism in the endometrium of women with PCOS differs from that observed in the normal endometrium (Bacallao et al, 2008; Leon et al, 2008). In the endometrium of PCOS women, Bacallao et al (2008) showed a decreased relationship between the activities of steroid sulfatase (STS) and estrogen sulfotransferase (ETS), whereas Leon et al (2008) found an increase in STS activity and a decrease in ETS. Bacallao et al (2008) also described an increased ratio between the mRNAs of 17β-hydroxysteroid dehydrogenase *(Hsd17b*) types 1 and 2 in the endometrium of PCOS women *versus* the normal endometrium. In another study, Margarit et al (2010) found that the HSD17B1 and HSD17B2 levels in anovulatory PCOS patients were significantly higher than those in fertile women. Regarding aromatase, results are contradictory. Some researchers have reported that aromatase is undetectable in the endometrium of PCOS and normal women (Bacallao et al, 2008; Leon et al, 2008), whereas others have shown that the levels of endometrial aromatase in PCOS patients are higher than those in normal women (Zhao et al, 2014).

Changes in steroid metabolism in the endometrium may alter the expression of hormone-responsive genes associated with uterine development and differentiation, such as homeobox gene A10 (*Hoxa10*), phosphatidylinositol 3, 4, 5-trisphosphate 3-phosphatase (*Pten*), wingless-related MMTV integration site member 5a and 7a (*Wnt5a* and *Wnt7a*) and β-catenin (*Ctnnb1*) (Mutter et al, 2000, Cermik et al, 2003, Al Naib et al, 2016). Regarding *Hoxa10*, endometrial biopsies from women with PCOS have demonstrated decreased *Hoxa10* (Cermik et al, 2003; Kara et al, 2019). Regarding PTEN, although a common finding in endometrial cancer or endometrial hyperplasia is the loss of PTEN

gene expression (Djordjevic et al, 2012; Yang et al, 2015), Shafiee et al (2016) found a significant up-regulation in PCOS women with endometrial cancer. Regarding the members of the Wnt family, studies in a PCOS rat model have shown that *Wnt4*, *Wnt5a*, and *Wnt7a* are not modified in the uterus, whereas, in PCOS women, some authors have shown a higher expression of *Wnt3* as well as of *Ctnnb1* (Mehdinejadiani et al, 2019; Zhang et al, 2017).

In a PCOS rat model, we have recently demonstrated an increase in uterine thickness and water content and alterations in collagen remodeling, cell proliferation and apoptosis (Bracho et al. 2019). These abnormalities were associated with modified expression of aquaporins, Insulin-like Growth Factor-I (*Igf1*), PTEN and steroid receptors (Bracho et al, 2020). In this study, employing the same animal model, our objective was to examine histomorphological uterine lesions in the luminal and glandular epithelium. Additionally, we aimed to assess tissue steroid pathways by measuring steroid levels, the enzymes responsible for steroidogenesis, and their specific receptors. Furthermore, we evaluated hormone-responsive genes associated with uterine differentiation and function. To explore the potential involvement of the androgen pathway in the uterine lesions of PCOS rats, we included a group treated with flutamide (F), which acts as an androgen receptor (AR) blocker.

2. MATERIALS AND METHODS

2.1 Animals and experimental design

The experimental protocols were designed in accordance with the Guide for the Care and Use of Laboratory Animals issued by the U.S. National Academy of Sciences (National Research Council Committee for the Update of the Guide for the Care and Use of

Laboratory Animals, 2011) and were approved by the Ethics Committee of the Facultad de Bioquímica y Ciencias Biológicas on 5 November 2019 (Resolution CE2019-47, FBCB, Universidad Nacional del Litoral, Santa Fe, Argentina).

Rats of a Wistar-derived strain inbred at the Department of Human Physiology (FBCB-UNL) were kept in a controlled environment (22 ± 2ºC; 14 h of light from 0500 to 1900) with free access to pellet laboratory chow (Nutrición Animal, Argentina). Rats were housed in stainless steel cages with sterile pine wood shavings as bedding. Tap water was supplied *ad libitum* in glass bottles with rubber stoppers.

A rat model mirroring key features observed in women with PCOS was developed through the injection of dehydroepiandrosterone (DHEA), and this model was utilized in our study (Lee et al, 2016, Zheng et al, 2022). At 21 days old, rats were randomly assigned to three groups (n= 7-11 in each group) and subcutaneously administered either sesame oil (Control group), DHEA (60 mg/kg body weight [bw]) (PCOS group) or DHEA (60 mg/kg bw) combined with flutamide (an AR antagonist, 20 mg/kg bw) (PCOS-F group) for 20 consecutive days (Bracho et al, 2020). Euthanasia occurred 24 h after the final DHEA or flutamide injection, and during autopsy, trunk blood and uterus were collected.

2.2 Hormone assays

Serum testosterone (T), E2 and P4 levels were determined by chemiluminescence assays, using an Immulite® 2000 system for *in vitro* diagnostics (Siemens Healthcare SA, Argentina) and following the manufacturer's specifications (Bracho et al, 2019). The intra-assay coefficient of variation was 6.7% for E2, 10.1% for T, and 9.7% for P4.

For the determination of uterine steroids, uterus tissue samples from nine rats per group were combined into three pools. The different pools were used to measure T, E2, P4 and

estrone (E1) as previously described by Gomez et al (2023). The tissue was homogenized in 1.0mL of methanol using an Ultra-Turrax homogenizer (T25 basic, IKA-Werke GMBH & Co. KG, Germany). The homogenate was centrifuged and the methanolic supernatant was separated. Then, chloroform was added to the pellet, which was mechanically shaken and centrifuged. The supernatant was taken and merged with the methanolic supernatant. Finally, the extract was dried under a gentle nitrogen stream and then reconstituted in H_2O: acetonitrile (50:50) and injected into the chromatographic system.

The chromatographic analysis was carried out using an LC1260 Agilent instrument equipped with a degasser, a binary pump, an auto-sampler, an oven column compartment, an UV-Vis diode array detector, a fast-scanning fluorescence detector, and the OpenLAB LC ChemStation software (Agilent Technologies, Waldbronn, Germany). The separation was performed on a 3.5 µm Zorbax Eclipse XDB-C18 analytical column (100 mm × 4.6 mm) (Agilent Technologies). The mobile phase consisted of a mixture of H_2O (solvent A) and acetonitrile (solvent B). The detection was performed by recording the UV spectra of T, E1 and P4 and the fluorescence emission spectra of E2 by using a λexc=317 nm. The data acquired were then chemometrically analyzed through Multivariate Curve Resolution-Alternating Least Squares. The limit of quantification of the method for E1, E2, T and P4 was 26.7 µg/L, 2.77 µg/L, 1.20 µg/L and 7.96 µg/L, respectively.

2.3 Histology and morphometry

Uterine samples embedded in paraffin were cut into 5-µm sections, mounted on slides coated with 3-aminopropyl triethoxysilane (Sigma–Aldrich, Argentina) and stained with hematoxylin and eosin or periodic acid–Schiff (PAS) for light microscopy (Olympus BH2, Tokyo, Japan). PAS staining was used in histochemistry to detect mucopolysaccharides in uterus (Demacopulo and Kreimann, 2019). Uterine glands were

199 classified as described by Vigezzi et al (2015). To assess the incidence of epithelial or
200 glandular abnormalities, the number of rats with at least one abnormality of the types
201 described was divided by the total number of rats per group (the result was expressed as
202 percentage). To evaluate luminal epithelial cell height and glandular density, three uterine
203 sections per animal were assessed, and at least 10 images were recorded in each section
204 with a Spot Insight V3.5 color video camera (Diagnostic Instruments, Sterling Heights,
205 MI, USA) attached to an Olympus BH2 microscope. The luminal epithelial cell height
206 was measured from the apical (luminal) surface to the basement membrane, as previously
207 described (Bracho et al, 2019). Areas with luminal hyperplasia were not included in this
208 quantification. To determine the glandular density, the area occupied by the uterine glands
209 was determined and referenced to the subepithelial stroma area by using the Image-Pro
210 Plus 4.1.0.1 system (Media Cybernetics, Silver Spring, MD, USA).

211 *2.4 Immunohistochemistry (IHC)*

212 Uterine sections (5 μm thick) were immunostained to detect the expression of aromatase,
213 estrogen alpha, beta and androgen receptors (ESR1, ESR2 and AR), WNT5a, WNT7a, β-
214 catenin, HOXA10 and PTEN, as previously described (Bracho et al, 2019). Primary
215 antibodies were incubated overnight at 4°C. The antibodies used were: anti-aromatase
216 (dilution 1:100, Instituto de Salud y Ambiente del Litoral (ISAL), Santa Fe, Argentina,
217 Gomez et al, 2023), anti-ESR1 (dilution 1:200, ISAL, Gomez et al, 2023), anti-ESR2 (cat
218 # 51-7900, dilution 1:50, Zymed, Thermo Fisher Scientific. AR), anti-AR (cat # sc-816,
219 dilution 1:400, Santa Cruz Biotechnology Inc. CA), anti-PTEN (dilution 1:750, ISAL,
220 Bracho et al, 2020), anti-WNT5a (dilution 1:200, ISAL, Vigezzi et al, 2016), anti-WNT7a
221 (dilution 1:400, ISAL, Vigezzi et al, 2016), anti-β-catenin (cat # sc-7963, dilution 1:800,
222 Santa Cruz Biotechnology Inc., Santa Cruz, CA, USA) and anti-HOXA10 (cat # sc-
223 17159, dilution 1:50, Santa Cruz Biotechnology Inc.). As secondary antibodies, anti-

mouse (dilution 1:200, ISAL, Gomez et al, 2023), anti-rabbit (dilution 1:200, ISAL, Bracho et al, 2020) and anti-goat (cat # sc-2042, dilution 1:100, Santa Cruz Biotechnology Inc.) were used. The reactions were developed using a streptavidin-biotin peroxidase method and diaminobenzidine (Sigma–Aldrich) as chromogen. Samples were mounted with a permanent mounting medium (Eukitt, Sigma-Aldrich). Each IHC run included negative controls in which the primary antibody was replaced by non-immune horse serum (Sigma–Aldrich).

Aromatase, ESR1, ESR2, AR and PTEN expression was quantified by measuring the integrated optical density (IOD). To measure the IOD immunostaining, at least 10 fields were recorded in each section, and three sections per animal were evaluated and analyzed using the Image-Pro Plus system (Media Cybernetics), as previously described by Varayoud et al (2011). The IOD was measured as a linear combination between average gray intensity and the relative area occupied by positive cells. Because the IOD is a dimensionless parameter, the results are expressed as arbitrary units.

2.5 Reverse transcription and real-time quantitative PCR analysis

Individual uterine horn samples were homogenized in TRIzol (Invitrogen, USA), and RNA was prepared according to the manufacturer's protocol. The concentration of total RNA was assessed by A260. Equal quantities (1 µg) of total RNA were reverse-transcribed into cDNA with Moloney Murine Leukemia Virus Reverse Transcriptase (10 units; Promega, USA) (Bracho et al, 2019).

The reverse-transcribed products were amplified in triplicate using the real-time PCR system StepOne Cycler (Applied Biosystems Inc., Life Technologies, Carlsbad, CA, USA). An optimized real-time PCR protocol was used to analyze the mRNA expression levels of enzymes that regulate steroid metabolism, *Esr1, Esr2, Pten, Wnt5a, Wnt7a,*

Ctnnb1, Hoxa10 and ribosomal protein L19 (RPL19). The *Rpl19* transcript was chosen as a housekeeping gene (internal control) following assessment of primer specificity and efficiency. Importantly, there were no statistically significant differences between the Ct values of the experimental groups (CONTROL: 23.74 ± 0.87; PCOS: 23.94 ± 0.44; PCOS-F: 23.47 ± 0.37). Primer sequences designed for cDNA amplification are described in Table 1. For cDNA amplification, a real-time PCR was performed using diluted cDNA combined with HOT FIREPol Eva Green qPCR Mix Plus (Solis BioDyne, Biocientífica, Argentina) and 0.5 pmol/µL of each primer (Invitrogen). After initial denaturation at 95°C for 15 min, the reaction mixture was subjected to successive cycles of denaturation at 95°C for 15 s, annealing at 55-60°C for 15 s, and extension at 72°C for 15 s. Product purity was confirmed by dissociation curves, and random samples were subjected to agarose gel electrophoresis. The relative expression levels of each target were calculated using the standard curve method (Bracho et al, 2019; Cikos et al, 2007).

2.6 Statistical analysis

Results are expressed as the mean ± SEM. The incidence of uterine abnormalities was analyzed by Fisher's exact test and post-hoc analysis. Luminal epithelial height, glandular density, relative gene expression and IOD were analyzed by one-way analysis of variance (ANOVA) and Bonferroni post-hoc tests or Kruskal-Wallis test followed by Dunn's post-hoc test. Values with $p < 0.05$ were accepted as significant difference between the groups. Analyses were carried out using the R software (The R Foundation for Statistical Computing, http://www.r-project.org/).

3. RESULTS

3.1 Uterine histomorphology

PCOS and PCOS-F rats presented several uterine alterations (Fig. 1). Both PCOS and PCOS-F rats showed a higher incidence of epithelial abnormalities than Control rats (Table 2). These rats presented areas with hyperplasia of the luminal epithelium, intraepithelial lumens positive to PAS staining, polyps, intraepithelial glandular formation, and increased luminal epithelial height (Fig. 1, Table 2). PCOS and PCOS-F rats also presented a higher incidence of abnormal glands (cystic glands, conglomerates of glands, glands with cellular atypia and glands with squamous metaplasia (Fig. 1, Table 2) and higher glandular density than Controls.

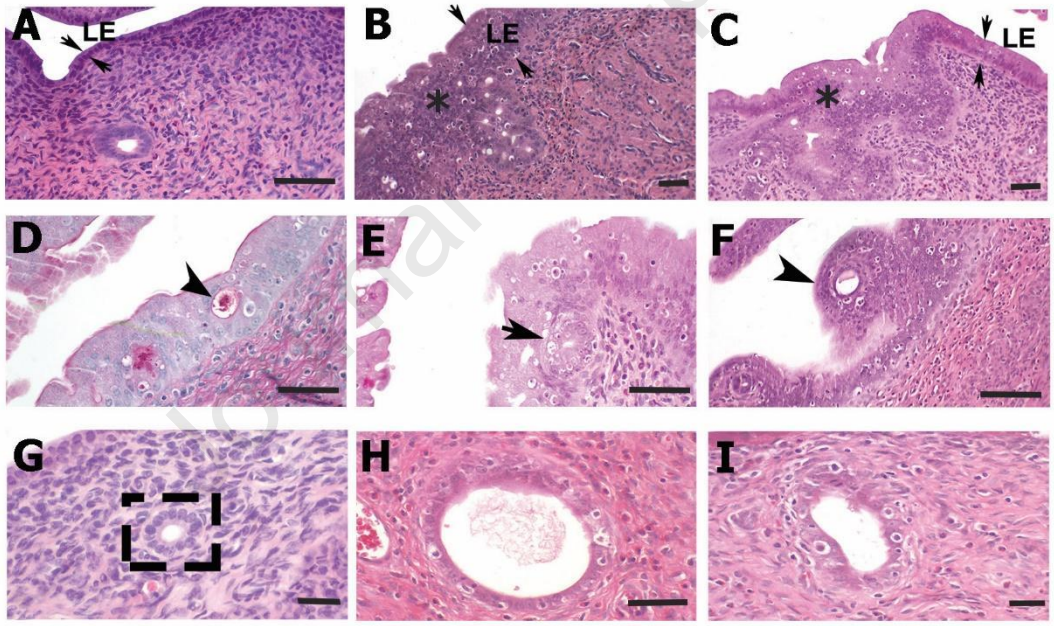

Figure 1: Representative photomicrographs of epithelial and glandular abnormalities observed in the uterus of polycystic ovary syndrome (PCOS) and PCOS-Flutamide (PCOS-F) rats on postnatal day 41 (PND41). (A) Normal luminal epithelium (LE), (B-C) luminal epithelium with hyperplasia (asterisk), (D) intraepithelial lumens (arrowhead), (E) intraepithelial gland formation (arrow), (F) polyps (arrowhead), (G) normal gland (box with dashed lines), (H) cystic gland and (I) gland with cellular atypia. The slides were stained with hematoxylin and eosin or periodic acid Schiff. Scale bar: 50 μm.

290 *3.2 Uterine endocrine status*

291 To investigate whether the alterations found in PCOS rats were associated with changes
292 in the uterine endocrine environment, serum and tissue steroid hormone levels, enzymes
293 involved in steroid metabolism, and steroid receptors expression were evaluated.

294 *3.2.1 Serum levels of steroids.* T was higher in PCOS and PCOS-F rats than in Controls.
295 E2 and P4 were similar between all groups (Table 3).

296 *3.2.2 Tissue levels of steroids.* The percentage of rats with steroid hormones detectable in
297 the uterus is shown in Table 3. No differences were found in the levels of hormones
298 between the groups: T (Control: 3.1±2.7, PCOS: not detected, PCOS-F 7.3 ± 2.2 µg/L),
299 E2 (Control: 5.1 ± 1.2, PCOS: 3.6 ± 0.4, PCOS-F 7.2± 1.4 µg/L), E1 (Control: 54.9 ±
300 38.1, PCOS: 55.7 ± 25.5, PCOS-F: 58.6 ± 31 µg/L) and P4 (Control: 56.2 ± 29.5, PCOS:
301 10.1 ± 1.8, PCOS-F: 56.1 ± 16.8 µg/L).

302 *3.2.3 Molecules related to steroid metabolism*. The following RNA transcripts that
303 regulate steroid metabolism were detected in the uterine tissue of all groups (Fig. 2): acute
304 regulatory protein (*Star*), 3α-hydroxysteroid dehydrogenase (*Akr1c14*), 3β-
305 hydroxysteroid dehydrogenase (*Hsd3b*, isoforms 1, 2, 3, 5 and 7), 17β-hydroxysteroid
306 dehydrogenase (*Hsd17b*, isoforms 1, 2, 3 and 4), steroid 5α-reductase type 1 (*Srd5a1*),
307 cytochrome P4502D4 (*Cyp2d4*), aromatase (*Cyp19a1*) and steroid sulfatase (*Sts*). No
308 expression of *Srd5a2* or cytochrome P45017A1 (*Cyp17a1*) was found. PCOS rats showed
309 a decrease in *Star* and an increase in *Hsd17b2*, *Cyp19a1* and *Srd5a1*. PCOS-F rats showed
310 the same changes as those described in PCOS rats regarding *Star*, *Hsd17b2* and *Srd5a1*;
311 however, the increase in *Cyp19a1* found in PCOS rats was not observed in PCOS-F ones
312 (Fig. 2).

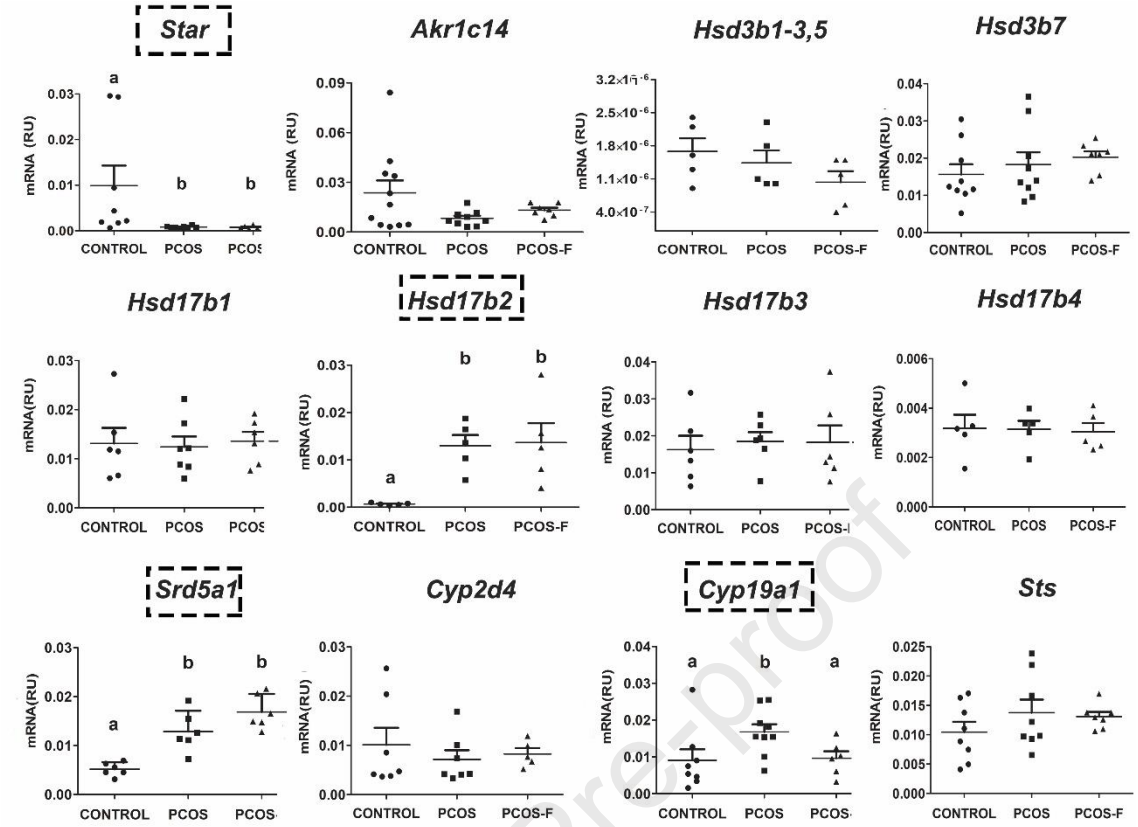

313

314 **Figure 2:** Quantification of mRNA by RT-PCR, performed on proteins involved in
315 regulating steroid metabolism in the uterus of PCOS and PCOS-F rats on PND41. The
316 mRNA levels of steroidogenic enzymes, indicated by dash rectangles, show significant
317 differences between experimental groups. It should be noted that no expression of *Srd5a2*
318 and *Cyp17a1* was detected in the rat uterus (data not shown). To normalize the samples,
319 mRNA of *Rpl19* was used as a housekeeping gene. The relative units (RU) of mRNA
320 expression were calculated. Each column in the graph represents the mean±SEM of 5-11
321 rats/group. All outliers were included in the analysis. Different letters are used to indicate
322 significant differences ($p < 0.05$, Kruskal-Wallis followed by Dunn's Multiple
323 Comparison post-test).

324

325 Aromatase immunostaining was present in the luminal and glandular epithelium,
326 subepithelial stroma and myometrium cells of Controls (Fig. 3). In PCOS rats, aromatase
327 increased in the luminal epithelium, but, in PCOS-F rats, it was similar to that of Controls
328 (Fig. 3). In the glandular epithelium of PCOS-F rats, aromatase was lower than in that of

PCOS rats (Fig. 3). In the subepithelial stroma and myometrium, no significant differences in aromatase immunostaining were observed between groups (Fig. 3).

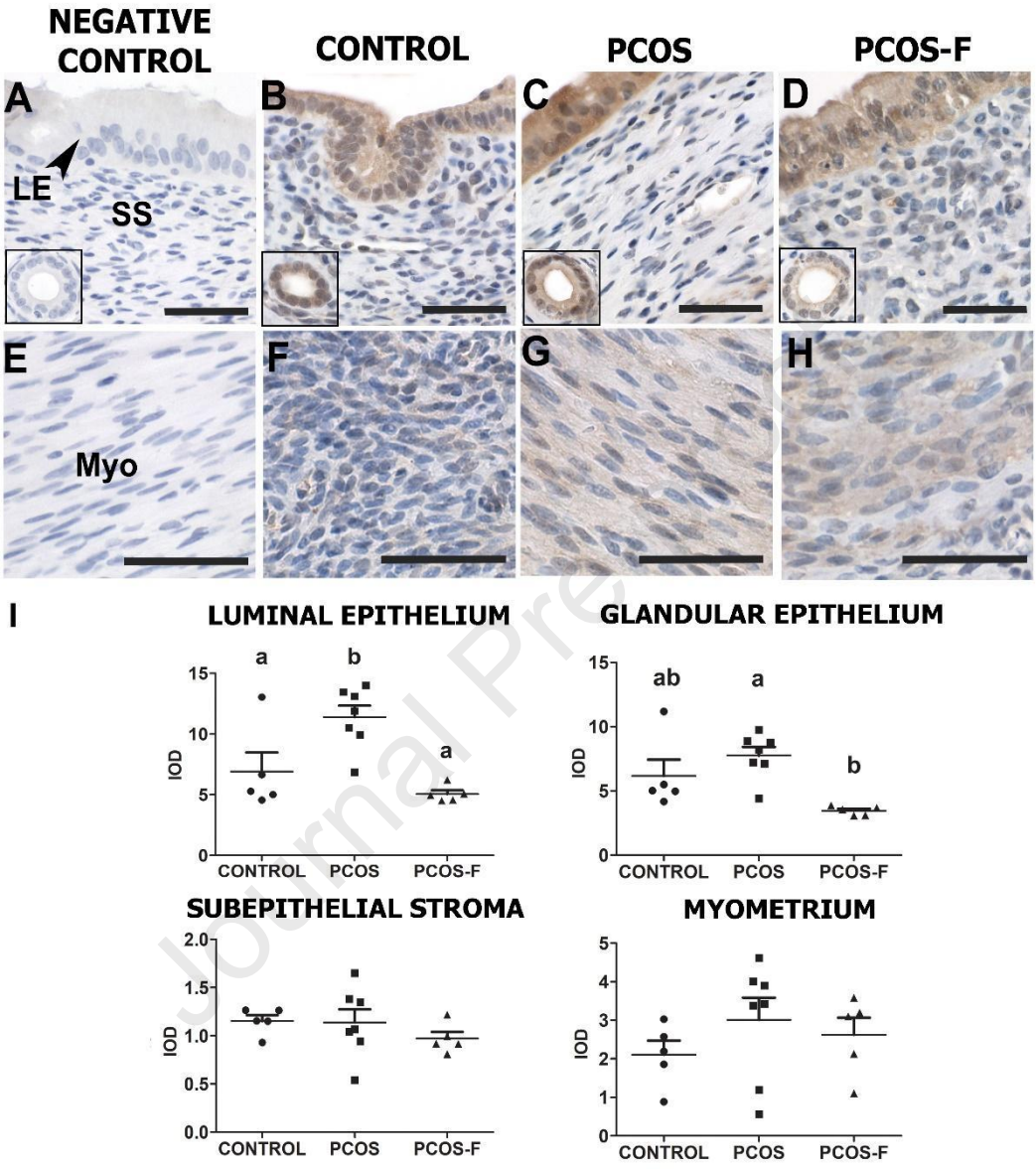

Figure 3: Immunohistochemical analysis of aromatase, conducted to assess its expression in the uterus of PCOS and PCOS-F rats on PND41. Immunostaining was observed in various uterine compartments, including the luminal epithelium (LE), glandular epithelium (inset), subepithelial stroma (SS) and myometrium (Myo). (A-E) The negative control was an immunostained uterine section of PCOS rats. Immunostained sections were counterstained with Mayer hematoxylin. Scale bar: 50 μm. (I) Quantification of aromatase immunostaining in different uterine compartments. Each column represents the mean±SEM of 5-7 rats/group. All outliers were included. Different letters are used to

indicate significant differences ($p < 0.05$; Kruskal-Wallis followed by Dunn's Multiple Comparison post-test). IOD: Integrated optical density.

A summary of the results concerning uterine tissue steroid levels and their metabolic pathways in the experimental groups is depicted in Fig. 4.

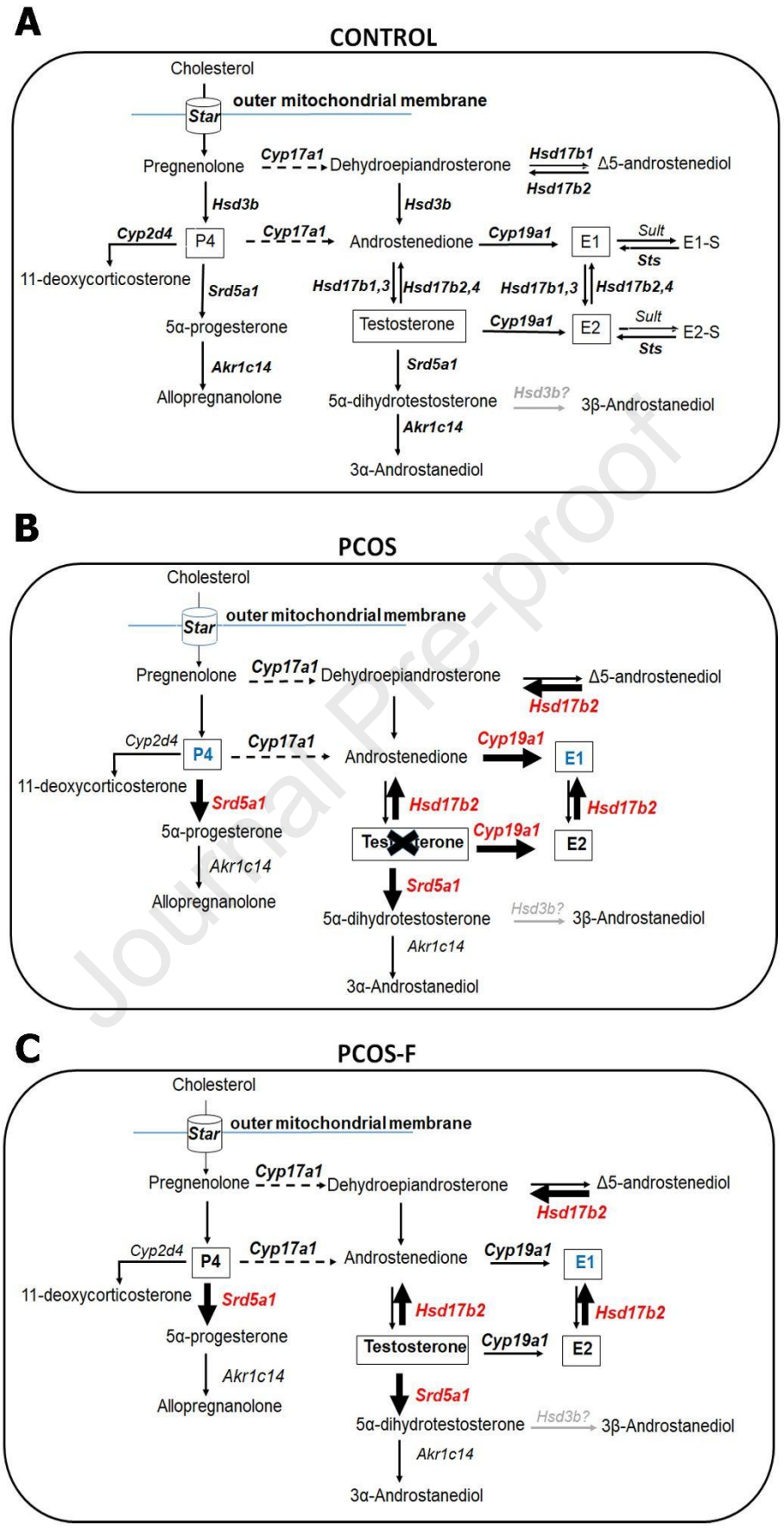

345

Figure 4: Hormonal microenvironment in the uterine tissue of rats on PND41. The pathways involved are indicated by arrows, and the uterine steroid hormones evaluated are highlighted with a box. Additionally, the enzymes that regulate steroid metabolism and were detected in the uterine tissue are included. No mRNA expression of *Cyp17a1* was detected in the uterus (indicated by arrows with dashed lines). Figure A represents the control conditions, showing the normal hormonal microenvironment in the uterine tissue. Figures B and C depict the modifications found in metabolic pathways, the mRNA expression of steroidogenic enzymes, and steroid hormones detected in the uterine tissue of PCOS and PCOS-F rats, respectively. In PCOS rat uterus, testosterone (T) was undetectable (indicated by a black cross), and the percentage of rats with detectable levels of progesterone (P4) and estrone (E1) was decreased (indicated in blue). The mRNA expression of *Star* was decreased (indicated by a thin black arrow), while the mRNA expression of *Srd5a1*, *Hsd17b2* and *Cyp19a1* was increased (indicated by a thickened black arrow). Additionally, PCOS rats showed increased expression of aromatase protein (indicated by a thickened black arrow). In the PCOS-F rat uterus, the percentage of rats with detectable T and P4, and the mRNA expression of *Cyp19a1* were similar to those of control rats. In uterine tissue of PCOS-F rat, E1 was decreased (indicated in blue). E2: 17β-estradiol. *Hsd3b?*: indicates that the reaction could be mediated by this enzyme.

3.2.4 Expression of estrogen and androgen receptors

In the uterus, both mRNA and ESR2 protein expression were lower in PCOS and PCOS-F rats compared to Control rats (Table 3). *Esr1* expression remained similar across all experimental groups, while a decreased in protein expression was observed in PCOS-F rats (Table 3). *Ar* expression increased in PCOS rats compared to Control group; however, this change was not observed in PCOS-F rats (Table 3). In the uterine subepithelial stroma, the expression pattern of AR protein showed a similar change to observed in *Ar*; however, in the myometrium of PCOS rats, protein levels increased, while in PCOS-F rats this increase was not statistically different compared to PCOS or Control rats (Table 3).

3.3 Molecules involved in uterine differentiation

Molecules responsible for uterine differentiation (i.e.: WNT5a, WNT7a, β-catenin, HOXA10 and PTEN) were next investigated in the uterine tissue of experimental groups. Gene expression was quantified using qRT-PCR, while protein levels was assessed via IHC to identify the specific cell and tissue compartment in which each protein is expressed, providing a qualitative assessment.

Wnt5a expression in PCOS and PCOS-F rats was similar but lower than that in Controls (Fig. 5A). WNT5a protein was present in the uterine luminal and glandular epithelium of Controls (Fig. 5B), but lower expression was found in the subepithelial stroma and myometrium. In PCOS and PCOS-F rats, WNT5a immunostaining decreased in all uterine compartments (Fig. 5B), accompanying the pattern of mRNA.

Wnt7a expression was similar in the three groups (Fig. 5A). WNT7a protein was present in all uterine compartments of Controls and did not change in PCOS or PCOS-F rats (Fig. 5B).

Ctnnb1 was higher in PCOS rats than in Controls, whereas PCOS-F rats showed no differences *versus* PCOS rats or Controls (Fig. 5A). β-catenin protein expression was found in the membrane of luminal and glandular epithelial cells in all groups (Fig. 5B), showing the same pattern as mRNA.

Hoxa10 was similar between Control and PCOS rats but lower in PCOS-F rats (Fig. 5A). In Controls, HOXA10 immunostaining was found in the uterine subepithelial stroma and myometrium, but its intensity was lower in the luminal and glandular epithelium (Fig. 5B). In PCOS-F rats, HOXA10 immunostaining decreased in the myometrium, as well as in the subepithelial stroma, although to a lesser extent.

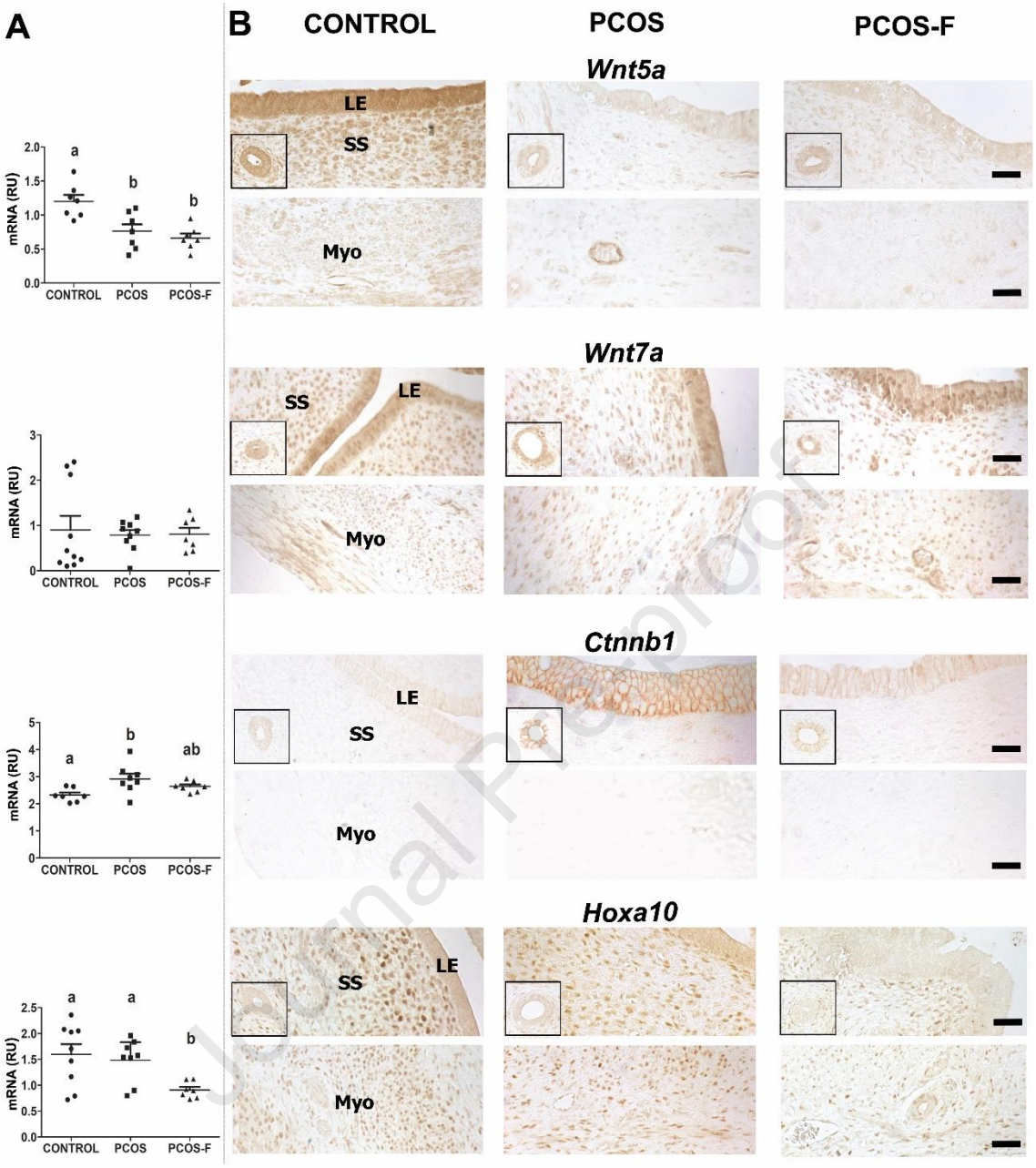

Figure 5: Protein and mRNA expression levels of WNT5a, WNT7a, β-catenin, and HOXA10, assessed in the uterus of PCOS and PCOS-F rats on PND41. (A) The mRNA levels of Wnt5a, Wnt7a, Ctnnb1 and Hoxa10 mRNA were quantified using RT-PCR in the uterus. The mRNA levels were normalized to the expression of *Rpl19*, which served as a housekeeping gene. Relative units (RU) were used. Each column represents the mean ± SEM of 7-10 animals/group, and all outliers were included. Different letters are used to indicate significant differences ($p < 0.05$; Kruskal-Wallis followed by Dunn's Multiple Comparison post-test). IOD: Integrated optical density. (B) Representative photomicrographs of uterine sections immunostained for WNT5a, WNT7a, β-catenin,

and HOXA10. The expression of these proteins were examined on different compartments of the uterus, including the luminal epithelium (LE), glandular epithelium (inset), subepithelial stroma (SS), and myometrium (Myo). Scale bar: 50 μm.

Pten was similar between the experimental groups (Fig. 6A). PTEN protein expression was detected in the luminal and glandular epithelium, subepithelial stroma and myometrium of all groups (Fig. 6B). In PCOS and PCOS-F uterine tissue, PTEN immunostaining decreased in the luminal epithelium, subepithelial stroma and myometrium compared with Control rats, whereas, in the glandular epithelium, PTEN protein expression was similar between groups (Fig. 6C).

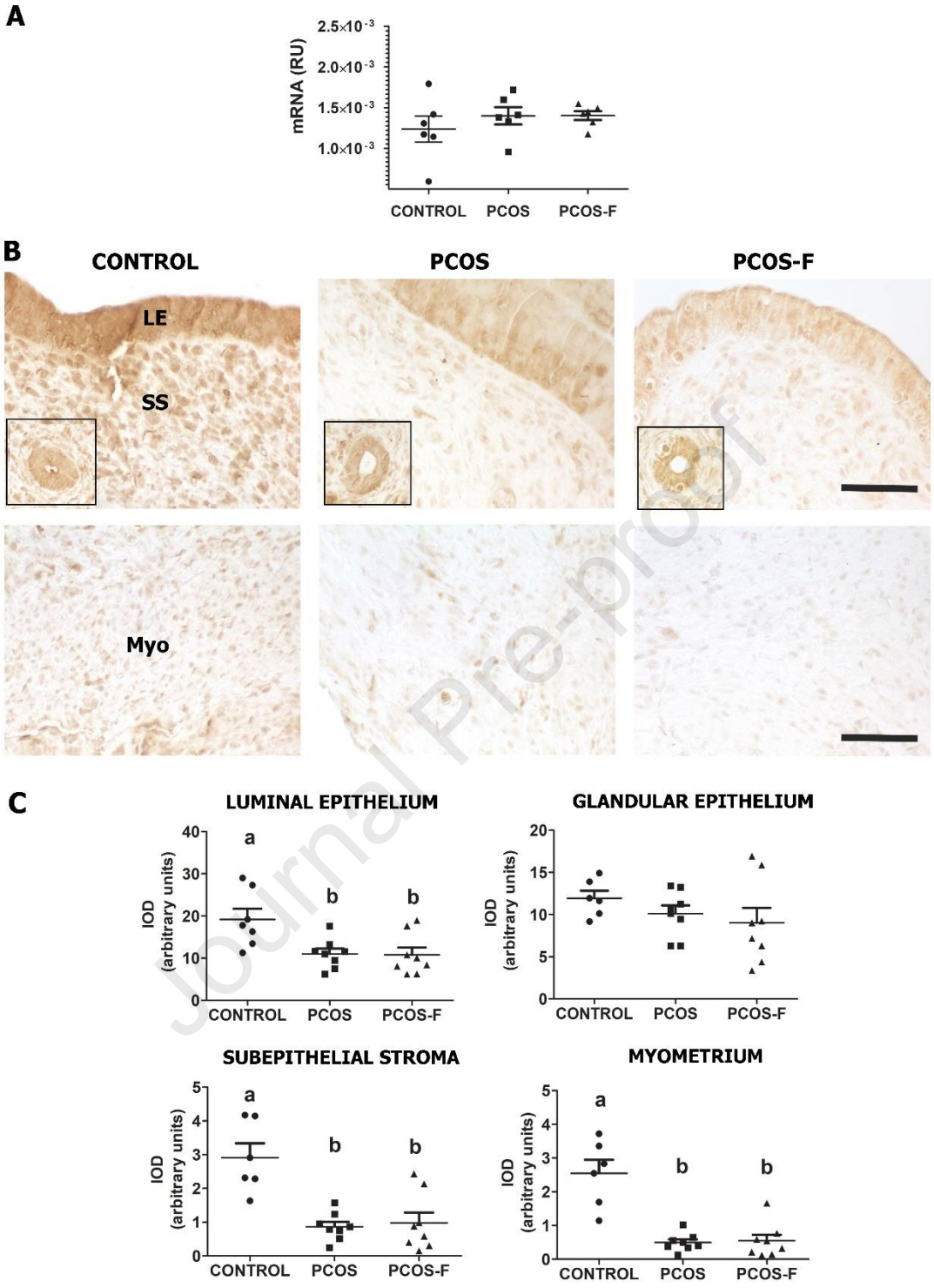

418

419 **Figure 6**: Protein and mRNA expression levels of PTEN in the uterus of PCOS and
420 PCOS-F rats on PND41. (A) PTEN mRNA was quantified using RT-PCR. The mRNA
421 levels were normalized to the expression of *Rpl19*, which served as a housekeeping gene.
422 RU: relative units. (B) Photomicrographs display uterine sections that were
423 immunostained for PTEN. This protein was expressed in the luminal epithelium (LE),

glandular epithelium (inset), subepithelial stroma (SS) and myometrium (Myo). Scale bar: 50 µm. (C) PTEN immunostaining was quantified in different compartments of the uterus. Each column represents the mean±SEM of 6-8 rats/group. All outliers were included. Different letters are used to indicate significant differences ($p < 0.05$; Kruskal-Wallis followed by Dunn's Multiple Comparison post-test). IOD: Integrated optical density.

4. DISCUSSION

PCOS is a known risk factor for uterine lesions, endometrial hyperplasia, and cancer. In this study, we have demonstrated several alterations in the luminal epithelium and gland morphology, in addition to those previously described in the subepithelial stroma and myometrium in a PCOS rat model (Bracho et al, 2020). Hyperplasia in the luminal epithelium and intraepithelial glands is known to be induced by estrogen exposure and a lack of P4 (Tokmak et al, 2014; Li et al, 2014). Intraepithelial lumens have been previously observed in rats treated with aromatizable androgens and have been associated with an increased expression of ezrin, a protein involved in the progression and metastasis of hormone-dependent tumors, in cells lining the lumens (Demacopulo & Kreimann, 2019; Xi & Tang, 2020). Within the uterine glandular compartment, Cystic glands are considered benign lesions, while the remaining structures (glands with squamous metaplasia, glands with cellular atypia, gland conglomerates, and glands with daughter glands) are regarded as pre-neoplastic lesions (Dixon et al, 2014). Previous studies have described these types of glandular abnormalities in adult rats (older than one year) and have shown that their incidence increases when rats receive estrogen treatment (Vigezzi et al, 2015). The high incidence of uterine epithelial and glandular lesions in both PCOS and PCOS-F rats suggests that these lesions may be linked to an endocrine environment deregulation.

The uterine endocrine environment is influenced by both serum hormone levels and the tissue availability of steroids (Plaza-Parrochia et al, 2017). Tissue hormone levels are linked to the expression and activity of steroidogenic enzymes (Gibson et al, 2018). Hasegawa et al. (2017) demonstrated that exposure of rat granulosa cells to 5α-dihydrotestosterone (DHT) and *Igf1* increased *Star* expression, while aromatase remained unaltered. In zebrafish embryos, both T and DHT up-regulated *Cyp19a1b* (an aromatase isoform) through an ESR-dependent pathway. The effects of T primarily involve aromatization, whereas DHT effect involves its conversion into 5α-androstan-3β, 17β-diol (3β-diol) (Mouriec et al, 2009). The findings concerning aromatase in uterine tissue are conflicting. Some studies report undetectable aromatase in the endometrium of women with or without PCOS (Leon et al, 2008; Bacallao et al, 2008), while others, such as Zhao et al. (2014), found higher expression of this enzyme in PCOS women's endometrium. In terms of other steroidogenic enzymes, some studies have shown that endometrial cells of PCOS women have higher HSD17B1 and HSD17B2 expression but lower ETS activity (Margarit et al, 2010). We observed decreased mRNA levels of *Star*, increased expression of *Hsd17b2*, *Srd5a1*, and *Cyp19a1*, and an absence of *Cyp17a1* in the uterus of PCOS rats, indicating that steroid hormones primarily originate from systemic hormonal metabolism rather than *de novo* synthesis. The absence of T in PCOS rats tissue may result from its conversion to androstenedione, DHT or E2, supported by the increased *Hsd17b2*, *Srd5a1*, and *Cyp19a1* expression. Additionally, DHT may be converted to 3β-diol, a metabolite with affinity for ESR2 (Abi Salloum et al, 2012; Handa et al, 2008). On the other hand, the lower levels of P4 in PCOS rat uterine tissue may be due to the increased expression of *Srd5a1*, which metabolizes P4 to 5α-dihydroprogesterone (Fig. 7B). These results indicate that P4 is unable to counteract

estrogen stimulation effectively. In PCOS-F rats, no increase in *Cyp19a1* compared to PCOS rats was demonstrated, suggesting transcriptional regulation through the AR pathway (Fig. 7C). It is also possible that the AR pathway in PCOS-F rats regulates the protein expression and/or activity of HSD17B2 and SRD5A1 since uterine P4 and T were present in most rats, indicating that these hormones were poorly metabolized by these enzymes.

The uterine endocrine environment is also regulated by the expression of steroid receptors. In the uterus of PCOS rats, ESR2 expression decreased, while AR expression increased. Interestingly, in PCOS-F rats, ESR2 decreased, but the increase in AR expression was not observed. Additionally, in this group, the expression of ESR1 also decreased. This observation is in agrees with Knapczyk-Stwora et al. (2011), who observed a decrease in stromal ESR1 expression in uterus of pigs treated with FLU. These findings suggest that AR expression could be regulated through ESR2 and ESR1. Several authors have proposed that these receptors collaborate to regulate their expression in various cells of reproductive tracts. For instance, it has been reported that ESR2-knockout mice exhibit increased AR expression in both prostate and ovaries (Weihua et al, 2001; Cheng et al, 2002). Conversely, Weihua et al. (2002) demonstrated that in the uterus of rats treated with E2, stromal ESR1 and AR were induced, indicating a positive regulatory between them. Overall, these results suggest a positive interaction between the ESR1 and AR pathways and a negative regulation between ESR2 and AR.

In our study, we investigated the impact of PCOS and PCOS-F on the expression of hormone-dependent genes. PTEN, a tumor suppressor, is implicated in endometrial cancer (Singh & Bhartiya, 2022). PTEN expression in the endometrium can be regulated,

enhanced by estrogens during the follicular/proliferative phase (Mutter et al, 2000). Estrogens can also increase its stability by promoting phosphorylation on S380, T382, and T383 residues in the PTEN C-Tail (Vazquez et al, 2000; Scully et al, 2014). However, Bai et al (2021) showed that phosphorylation at single residue of T366 induces PTEN protein degradation via promotion of PTEN ubiquitination. Studies in prostate and breast cancer cell lines have suggested a positive regulation between ESR2 and PTEN expression (Wu et al, 2017; Lindberg et al, 2011). In PCOS and PCOS-F rats, we suggest post-translational modifications in the PTEN expression, possibly due to changes in the degree phosphorylations in the C-Tail region (Kotelevets et al, 2020, Bai et al, 2021). The reduced uterine ESR2 expression in PCOS and PCOS-F rats may be linked to decreased PTEN protein expression in the stromal and luminal epithelium (Fig. 7B and C). Thus, decreased PTEN protein and elevated *Igf1*, previously shown in these animals (Bracho et al, 2020) may stimulate cell proliferation, potentially contributing to the observed uterine histomorphological changes in this PCOS model.

Previous studies, including our own, have highlighted the role of HOXA10 as a critical regulator of uterine stromal cell proliferation. Its expression is induced by both P4 and E2 (Lim et al, 1999; Varayoud et al, 2008; He et al, 2018). WNTs also play a crucial role in uterine stromal cell proliferation. Knockdown of *Wnt5a* in uterine stromal cell lines has been shown to inhibit stromal cell proliferation (Rider et al, 2016). Another study demonstrated that tamoxifen, an estrogen receptor agonist in the uterus, reduced *Wnt5a* transcript levels, associated with decreased *Esr2* expression in uterine tissue (Al Naib et al, 2016). Our findings indicate that the reduced ESR2 expression may be linked to decreased WNT5a expression, potentially leading to decreased uterine cell proliferation, consistent with our previous observations in the subepithelial stroma of PCOS and PCOS-

F rats (Bracho et al, 2019, 2020). Additionally, the observed decrease in ESR1 may contribute to a reduction in HOXA10 expression and uterine cell proliferation in PCOS-F (Bracho et al, 2019, 2020).

Our findings and suggested mechanism are summarized in Figure 7. In PCOS rats, changes in 3β-diol levels, a metabolite of DHT, may be involved in the down-regulation of uterine ESR2 expression. ESR2 could negatively regulate stromal AR expression, while ESR1 may have a positive regulatory role (Fig. 7B). The decrease in *Star* expression and the increase in *Hsd17b2*, *Srd5a1*, and *Cyp19a1* result in undetectable T levels in 100% of the animals and contribute to decreased P4 levels (Fig. 7B). As a result, the uterine hormonal environment differs from serum hormone levels (Fig. 7B). Reduced ESR2 expression may also play a role in the decreased PTEN expression in the luminal epithelium and stroma. When combined with higher *Igf1* expression, this has the potential to increase the development of epithelial and glandular lesions in our PCOS model. Additionally, reduced *Wnt5a* expression could contribute to decreased proliferation in subepithelial stromal cells (Fig. 7B).

In PCOS-F rats, we observed uterine lesions similar to those in PCOS rats. Notably, T was detected in uterine tissue, and more PCOS-F rats had detectable P4 levels compared to PCOS rats. Furthermore, PCOS-F rats exhibited a decrease in ESR1, a partial increase in AR, and no increase in aromatase expression. This suggests that aromatase expression may be regulated directly or indirectly through AR, possibly associated with ESR1 expression. Additionally, a decrease in WNT5a and HOXA10 was observed, potentially contributing to the reduced proliferation of the subepithelial stroma and myometrium, as previously demonstrated (Fig. 7C).

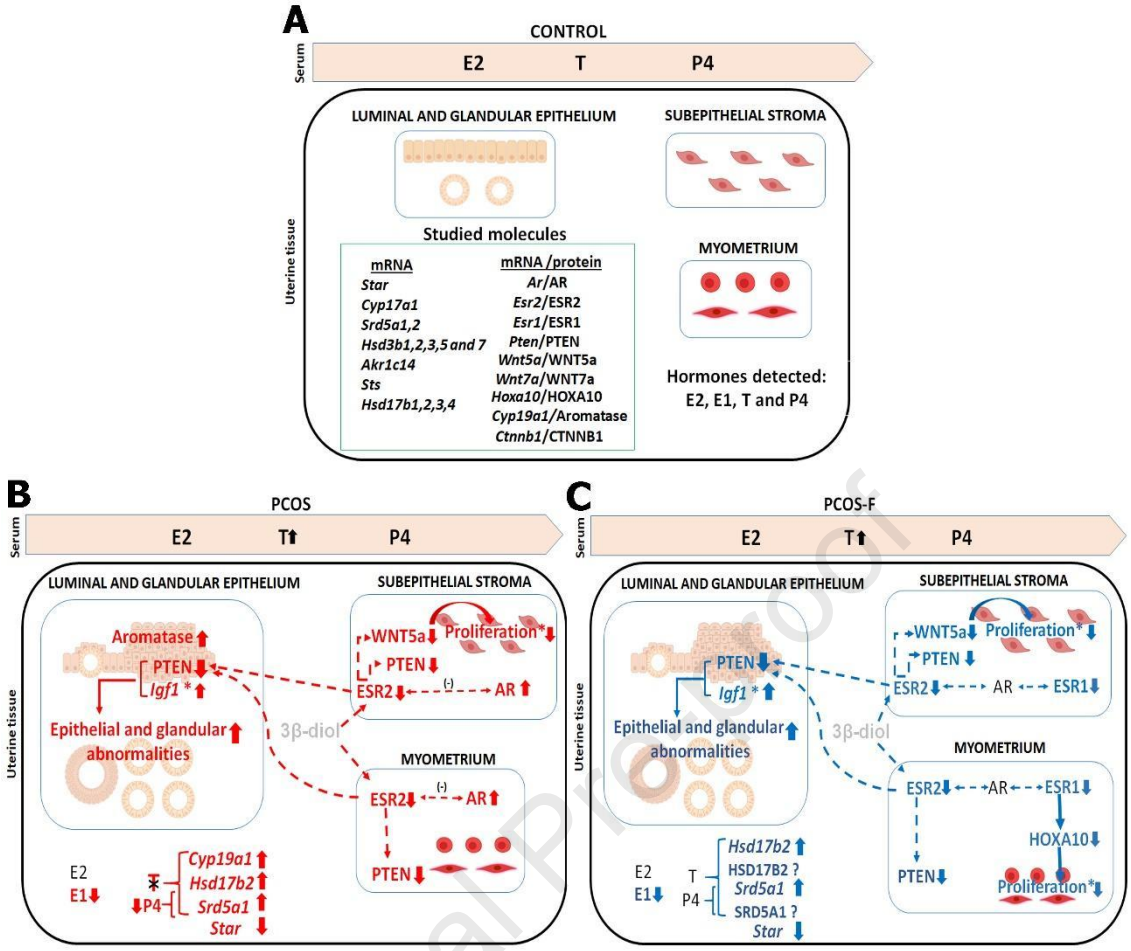

Figure 7: Summary and interpretation of the results. Figure A shows the steroids studied and the molecules evaluated in the uterine tissue of control rats. Figures B and C show the changes observed in PCOS and PCOS-F respectively. Black letters indicate no differences compared to the control group. Down or up arrows indicate decreased or increased expression/detection, respectively. Dashed arrows indicate the suggested pathway of interaction between molecules. In both PCOS and PCOS-F rats, the serum levels of T were higher than in the control group (B-C). In PCOS rats (Figure B), the uterine tissue showed undetectable levels of T could be associated with lower expression of *Star* and higher of expression of *Hsd17b2* and *Srd5a1*. Possible changes in the 3β-diol level may be involved in the down-regulation of stromal ESR2 expression. In the subepithelial stroma and myometrium, we suggest an inverse regulation (-) between ESR2 and AR. The lower ESR2 expression could be down-regulate the PTEN and WNT5a expression. The altered histomorphology of the luminal and glandular epithelium are associated with decreased PTEN expression and increased *Igf1* expression. In the subepithelial stroma, WNT5a expression is decreased in association with decreased cell proliferation. Different to PCOS, in PCOS-F rats (Figure C), we suggest that the

interaction between AR and ESR1 is altered, which modified aromatase expression. Furthermore, the decrease in HOXA10 is associated with a reduction in ESR1 in the myometrium, which also can contribute to the decrease in cell proliferation. (*): Results obtained from Bracho et al, 2020. P4: progesterone, E1: estrone, T: testosterone, E2: 17β-estradiol.

In conclusion, the results presented here demonstrate that the primary cause of the uterine lesions and histomorphological changes observed in PCOS is the alterations in tissue steroid metabolism and the cross-talk between steroid receptors.

5. FUNDING

This work was supported by grants from Agencia Nacional de Promoción Científica y Tecnológica (ANPCyT, PICT 2016 N° 0390, PICT 2019 N°1768), Consejo Nacional de Investigaciones Científicas y Técnicas (CONICET, PIP 2020 N°1387) and Universidad Nacional del Litoral (UNL, CAID 2020 PIC 50620190100026LI), Argentina. These funding sources were not involved in the study design, collection, analysis or interpretation of the data, the writing of the report, or the decision to submit the article for publication.

6. DECLARATION OF CONFLICTING INTERESTS

None.

7. ACKNOWLEDGEMENTS

We thank Walter Nykolajczuk and Juan Grant, for technical assistance and animal care. G.S.B. and M.V.A. are fellows of the Consejo Nacional de Investigaciones Científicas y Técnicas (CONICET) and G.A.A., M.R.A., M.M., M.J.C., M.F.R., L.K., E.H.L. and V.L.B. are Career Investigators of CONICET, Argentina.

8. REFERENCES

Abi Salloum, B., Herkimer, C., Lee, J.S., Veiga-Lopez, A. & Padmanabhan, V. (2012) Developmental programming: prenatal and postnatal contribution of androgens and insulin in the reprogramming of estradiol positive feedback disruptions in prenatal testosterone-treated sheep. Endocrinology. 153(6), 2813-2822. https://doi:10.1210/en.2011-2074

Al Naib, A., Tucker, H.L.M., Xie, G., Keisler, D.H., Bartol, F.F., Rhoads, R.P., Akers, R.M. & Rhoads, M.L. (2016) Prepubertal tamoxifen treatment affects development of heifer reproductive tissues and related signaling pathways. J Dairy Sci. 99(7), 5780-5792. https://doi:10.3168/jds.2015-10679

Bacallao, K., Leon, L., Gabler, F., Soto, E., Romero, C., Valladares, L. & Vega, M. (2008) In situ estrogen metabolism in proliferative endometria from untreated women with polycystic ovarian syndrome with and without endometrial hyperplasia. J Steroid Biochem Mol Biol. 110(1-2), 163-169. https://doi:10.1016/j.jsbmb.2008.03.031

Bai, D., Wu, Y., Deol, P., Nobumori, Y., Zhou, Q., Sladek, F.M. & Liu, X. (2021) Palmitic acid negatively regulates tumor suppressor PTEN through T366 phosphorylation and protein degradation. Cancer Lett, 496 127-133. https:// doi:10.1016/j.canlet.2020.10.007

Barry, J.A., Azizia, M.M. & Hardiman, P.J. (2014) Risk of endometrial, ovarian and breast cancer in women with polycystic ovary syndrome: a systematic review and meta-analysis. Hum Reprod Update. 20(5), 748-758. https://doi:10.1093/humupd/dmu012

Bermúdez Brito, M., Goulielmaki, E. & Papakonstanti, E.A. (2015) Focus on PTEN Regulation. Front Oncol. 5, 166. https://doi:10.3389/fonc.2015.00166

Bracho, G.S., Altamirano, G.A., Kass, L., Luque, E.H. & Bosquiazzo, V.L. (2019) Hyperandrogenism Induces Histo-Architectural Changes in the Rat Uterus. Reprod Sci. 26(5), 657-668. https://doi:10.1177/1933719118783881

Bracho, G.S., Acosta, M.V., Altamirano, G.A., Tschopp, M.V., Luque, E.H., Kass, L. & Bosquiazzo, V.L. (2020) Androgen receptor and uterine histoarchitecture in a PCOS rat model. Mol Cell Endocrinol. 518, 110973. https://doi:10.1016/j.mce.2020.110973

Cermik, D., Selam, B. & Taylor, H.S. (2003) Regulation of HOXA-10 Expression by Testosterone in Vitro and in the Endometrium of Patients with Polycystic Ovary Syndrome. J Clin Endocrinol Metab. 88(1), 238-243. https://doi:10.1210/jc.2002-021072

Cheng, G., Weihua, Z., Mäkinen, S., Mäkelä, S., Saji, S., Warner, M., Gustafsson, J.A. & Hovatta, O. (2002) A role for the androgen receptor in follicular atresia of estrogen receptor beta knockout mouse ovary. Biol Reprod. 66(1), 77-84. https://doi:10.1095/biolreprod66.1.77

Cheung, A.P. (2001) Ultrasound and menstrual history in predicting endometrial hyperplasia in polycystic ovary syndrome. Obstet Gynecol. 98(2), 325-331. https://doi:10.1016/s0029-7844(01)01432-6

Cikos, S., Bukovská, A. & Koppel, J. (2007) Relative quantification of mRNA: comparison of methods currently used for real-time PCR data analysis. BMC Mol Biol. 8, 113. https://doi:10.1186/1471-2199-8-113

Codner, E., Iñíguez, G.n., Villarroel, C., Lopez, P., Soto, N.s., Sir-Petermann, T., Cassorla, F. & Rey, R.A. (2007) Hormonal Profile in Women with Polycystic Ovarian Syndrome with or without Type 1 Diabetes Mellitus. J Clin Endocrinol Metab. 92(12), 4742-4746. https://doi:10.1210/jc.2007-1252

Demacopulo, B. & Kreimann, E.L. (2019) Bisphenol S increases EZRIN expression and the detrimental effects induced by dehydroepiandrosterone in rat endometrium. Mol Cell Endocrinol. 483, 64-73. https://doi:10.1016/j.mce.2019.01.006

Dixon, D., Alison, R., Bach, U., Colman, K., Foley, G.L., Harleman, J.H., Haworth, R., Herbert, R., Heuser, A., Long, G., Mirsky, M., Regan, K., Van Esch, E., Westwood, F.R., Vidal, J. & Yoshida, M. (2014) Nonproliferative and proliferative lesions of the rat and mouse female reproductive system. J Toxicol Pathol. 27(3-4 Suppl), 1s-107s. https://doi:10.1293/tox.27.1S

Djordjevic B., Hennessy B.T., Li J., Barkoh B.A., Luthra R., Mills G.B. & Broaddus R.R. (2012) Clinical assessment of PTEN loss in endometrial carcinoma: immunohistochemistry outperforms gene sequencing. Mod Pathol, 25 699-708. https://doi: 10.1038/modpathol.2011.208

669 Dumesic, D.A. & Lobo, R.A. (2013) Cancer risk and PCOS. Steroids. 78(8), 782-785.
670 https://doi:10.1016/j.steroids.2013.04.004

671

672 Gibson D.A., Simitsidellis I., Collins F. & Saunders P.T.K. (2018) Endometrial
673 Intracrinology: Oestrogens, Androgens and Endometrial Disorders. Int J Mol Sci, 19.
674 https:// doi:10.3390/ijms19103276

675

676 Gomez, A.L., Altamirano, G.A., Alcaraz, M.R., Montemurro, M., Schierano-Marotti, G.,
677 Oddi, S.L., Culzoni, M.J., Muñoz-de-Toro, M., Bosquiazzo, V.L. & Kass, L. (2023)
678 Mammary gland development in male rats perinatally exposed to propiconazole,
679 glyphosate, or their mixture. Environ Toxicol Pharmacol. 101, 104184.
680 https://doi:10.1016/j.etap.2023.104184

681

682 Handa, R.J., Pak, T.R., Kudwa, A.E., Lund, T.D. & Hinds, L. (2008) An alternate
683 pathway for androgen regulation of brain function: activation of estrogen receptor beta
684 by the metabolite of dihydrotestosterone, 5alpha-androstane-3beta,17beta-diol. Horm
685 Behav. 53(5), 741-752. https://doi:10.1016/j.yhbeh.2007.09.012

686

687 Haoula, Z., Salman, M. & Atiomo, W. (2012) Evaluating the association between
688 endometrial cancer and polycystic ovary syndrome. Hum Reprod. 27(5), 1327-1331.
689 https://doi:10.1093/humrep/des042

690

691 Hasegawa, T., Kamada, Y., Hosoya, T., Fujita, S., Nishiyama, Y., Iwata, N., Hiramatsu,
692 Y. & Otsuka, F. (2017) A regulatory role of androgen in ovarian steroidogenesis by rat
693 granulosa cells. J Steroid Biochem Mol Biol. 172, 160-165.
694 https://doi:10.1016/j.jsbmb.2017.07.002

695

696 He, B., Ni, Z.L., Kong, S.B., Lu, J.H. & Wang, H.B. (2018) Homeobox genes for embryo
697 implantation: From mouse to human. Animal Model Exp Med. 1(1), 14-22.
698 https://doi:10.1002/ame2.12002

699

700 Hosseinzadeh P., Barsky M., Gibbons W.E. & Blesson C.S. (2021) Polycystic Ovary
701 Syndrome and the Forgotten Uterus. F S Rev, 2 11-20.
702 https://doi:10.1016/j.xfnr.2020.12.001

703

704 Kaaks, R., Lukanova, A. & Kurzer, M.S. (2002) Obesity, endogenous hormones, and
705 endometrial cancer risk: a synthetic review. Cancer epidemiology, biomarkers &
706 prevention: a publication of the American Association for Cancer Research, cosponsored

by the American Society of Preventive Oncology, 11 (12), 1531-1543. https://api.semanticscholar.org/CorpusID:8795807

Kara, M., Ozcan, S.S., Aran, T., Kara, O. & Yilmaz, N. (2019) Evaluation of Endometrial Receptivity by Measuring HOXA-10, HOXA-11, and Leukemia Inhibitory Factor Expression in Patients with Polycystic Ovary Syndrome. Gynecol Minim Invasive Ther. 8(3), 118-122. https://doi:10.4103/gmit.Gmit_112_18

Kotelevets, L., Trifault, B., Chastre, E. & Scott, M.G.H. (2020) Posttranslational Regulation and Conformational Plasticity of PTEN. Cold Spring Harb Perspect Med, 10. https:// doi.org/10.1101/cshperspect.a036095

Knapczyk-Stwora, K., Durlej, M., Bilinska, B. & Slomczynska, M. (2011) Immunohistochemical studies on the proliferative marker Ki-67 and estrogen receptor alpha (ERα) in the uterus of neonatal and immature pigs following exposure to flutamide. Acta Histochem. 113(5), 534-541. https://doi:10.1016/j.acthis.2010.05.008

Lee, M.J., Jang, M., Bae, C.S., Park, K.S., Kim, H.J., Lee, S., Lee, S.W., Kim, Y.O. & Cho, I.H. (2016) Effects of Oriental Medicine Kyung-Ok-Ko on Uterine Abnormality in Hyperandrogenized Rats. Rejuvenation Res, 19 456-466. https:// doi.org/10.1089/rej.2015.1787

Leon, L., Bacallao, K., Gabler, F., Romero, C., Valladares, L. & Vega, M. (2008) Activities of steroid metabolic enzymes in secretory endometria from untreated women with Polycystic Ovary Syndrome. Steroids. 73(1), 88-95. https://doi:10.1016/j.steroids.2007.09.003

Li, X., Feng, Y., Lin, J.F., Billig, H. & Shao, R. (2014) Endometrial progesterone resistance and PCOS. J Biomed Sci. 21(1), 2. https://doi:10.1186/1423-0127-21-2

Lim, H., Ma, L., Ma, W.-g., Maas, R.L. & Dey, S.K. (1999) Hoxa-10 Regulates Uterine Stromal Cell Responsiveness to Progesterone during Implantation and Decidualization in the Mouse. Molecular Endocrinology. 13(6), 1005-1017. https://doi:10.1210/mend.13.6.0284

Lindberg, K., Helguero, L.A., Omoto, Y., Gustafsson, J. & Haldosén, L.A. (2011) Estrogen receptor β represses Akt signaling in breast cancer cells via downregulation of

HER2/HER3 and upregulation of PTEN: implications for tamoxifen sensitivity. Breast Cancer Res. 13(2), R43. https://doi:10.1186/bcr2865

Margarit, L., Taylor, A., Roberts, M.H., Hopkins, L., Davies, C., Brenton, A.G., Conlan, R.S., Bunkheila, A., Joels, L., White, J.O. & Gonzalez, D. (2010) MUC1 as a discriminator between endometrium from fertile and infertile patients with PCOS and endometriosis. J Clin Endocrinol Metab. 95(12), 5320-5329. https://doi:10.1210/jc.2010-0603

Mehdinejadiani, S., Amidi, F., Mehdizadeh, M., Barati, M., Pazhohan, A., Alyasin, A., Mehdinejadiani, K. & Sobhani, A. (2019) Effects of letrozole and clomiphene citrate on Wnt signaling pathway in endometrium of polycystic ovarian syndrome and healthy women†. Biol Reprod. 100(3), 641-648. https://doi:10.1093/biolre/ioy187

Mouriec, K., Gueguen, M.M., Manuel, C., Percevault, F., Thieulant, M.L., Pakdel, F. & Kah, O. (2009) Androgens upregulate cyp19a1b (aromatase B) gene expression in the brain of zebrafish (Danio rerio) through estrogen receptors. Biol Reprod. 80(5), 889-896. https://doi:10.1095/biolreprod.108.073643

Mutter, G.L., Lin, M.C., Fitzgerald, J.T., Kum, J.B., Baak, J.P., Lees, J.A., Weng, L.P. & Eng, C. (2000) Altered PTEN expression as a diagnostic marker for the earliest endometrial precancers. J Natl Cancer Inst. 92(11), 924-930. https://doi:10.1093/jnci/92.11.924

Nees L.K., Heublein S., Steinmacher S., Juhasz-Böss I., Brucker S., Tempfer C.B. & Wallwiener M. (2022) Endometrial hyperplasia as a risk factor of endometrial cancer. Archives of Gynecology and Obstetrics, 306 407-421. https://doi.org/10.1007/s00404-021-06380-5

Plaza-Parrochia F., Romero C., Valladares L. & Vega M. (2017) Endometrium and steroids, a pathologic overview. Steroids, 126 85-91. https://doi.org/10.1016/j.steroids.2017.08.007

Rider, V., Talbott, A., Bhusri, A., Krumsick, Z., Foster, S., Wormington, J. & Kimler, B.F. (2016) WINGLESS (WNT) signaling is a progesterone target for rat uterine stromal cell proliferation. J Endocrinol. 229(2), 197-207. https://doi:10.1530/joe-15-0523

781 Rotterdam ESHRE/ASRM-sponsored PCOS consensus workshop group. (2004) Revised
782 2003 consensus on diagnostic criteria and long-term health risks related to polycystic
783 ovary syndrome (PCOS). Hum Reprod. 19(1), 41-47. https://doi:10.1093/humrep/deh098

784

785 Shang K., Jia X., Qiao J., Kang J. & Guan Y. (2012) Endometrial Abnormality in Women
786 With Polycystic Ovary Syndrome, 19 674-683. https://doi: 10.1177/1933719111430993

787

788 Scully, M.M., Palacios-Helgeson, L.K., Wah, L.S. & Jackson, T.A. (2014) Rapid
789 estrogen signaling negatively regulates PTEN activity through phosphorylation in
790 endometrial cancer cells. Horm Cancer. 5(4), 218-231. https://doi:10.1007/s12672-014-
791 0184-z

792

793 Shafiee, M.N., Khan, G., Ariffin, R., Abu, J., Chapman, C., Deen, S., Nunns, D., Barrett,
794 D.A., Seedhouse, C. & Atiomo, W. (2014) Preventing endometrial cancer risk in
795 polycystic ovarian syndrome (PCOS) women: could metformin help? Gynecol Oncol.
796 132(1), 248-253. https://doi:10.1016/j.ygyno.2013.10.028

797

798 Shafiee, M.N., Seedhouse, C., Mongan, N., Chapman, C., Deen, S., Abu, J. & Atiomo,
799 W. (2016) Up-regulation of genes involved in the insulin signalling pathway (IGF1,
800 PTEN and IGFBP1) in the endometrium may link polycystic ovarian syndrome and
801 endometrial cancer. Mol Cell Endocrinol. 424, 94-101.
802 https://doi:10.1016/j.mce.2016.01.019

803

804 Singh, P. & Bhartiya, D. (2022) Molecular Insights into Endometrial Cancer in Mice.
805 Stem Cell Rev Rep. 18(5), 1702-1717. https://doi:10.1007/s12015-022-10367-3

806

807 Skiba, M.A., Islam, R.M., Bell, R.J. & Davis, S.R. (2018) Understanding variation in
808 prevalence estimates of polycystic ovary syndrome: a systematic review and meta-
809 analysis. Hum Reprod Update. 24(6), 694-709. https://doi:10.1093/humupd/dmy022

810

811 Tokmak, A., Kokanali, M.K., Guzel, A.I., Kara, A., Topcu, H.O. & Cavkaytar, S. (2014)
812 Polycystic ovary syndrome and risk of endometrial cancer: a mini-review. Asian Pac J
813 Cancer Prev. 15(17), 7011-7014. https://doi:10.7314/apjcp.2014.15.17.7011

814

815 Varayoud, J., Ramos, J.G., Bosquiazzo, V.L., Lower, M., Muñoz-de-Toro, M. & Luque,
816 E.H. (2011) Neonatal exposure to bisphenol A alters rat uterine implantation-associated
817 gene expression and reduces the number of implantation sites. Endocrinology. 152(3),
818 1101-1111. https://doi:10.1210/en.2009-1037

Varayoud, J., Ramos, J.G., Bosquiazzo, V.L., Muñoz-de-Toro, M. & Luque, E.H. (2008) Developmental exposure to Bisphenol a impairs the uterine response to ovarian steroids in the adult. Endocrinology. 149(11), 5848-5860. https://doi:10.1210/en.2008-0651

Vazquez, F., Ramaswamy, S., Nakamura, N. & Sellers, W.R. (2000) Phosphorylation of the PTEN tail regulates protein stability and function. Mol Cell Biol, 20 5010-8. https:// doi.org/10.1128/MCB.20.14.5010-5018.2000

Vigezzi, L., Ramos, J.G., Kass, L., Tschopp, M.V., Muñoz-de-Toro, M., Luque, E.H. & Bosquiazzo, V.L. (2016) A deregulated expression of estrogen-target genes is associated with an altered response to estradiol in aged rats perinatally exposed to bisphenol A. Mol Cell Endocrinol. 426, 33-42. https://doi:10.1016/j.mce.2016.02.010

Weihua, Z., Ekman, J., Almkvist, A., Saji, S., Wang, L., Warner, M. & Gustafsson, J.A. (2002a) Involvement of androgen receptor in 17beta-estradiol-induced cell proliferation in rat uterus. Biol Reprod. 67(2), 616-623. https://doi:10.1095/biolreprod67.2.616

Weihua, Z., Warner, M. & Gustafsson, J.A. (2002b) Estrogen receptor beta in the prostate. Mol Cell Endocrinol. 193(1-2), 1-5. https://doi:10.1016/s0303-7207(02)00089-8

Wu, C.W., Bell, R.A. & Storey, K.B. (2015) Post-translational regulation of PTEN catalytic function and protein stability in the hibernating 13-lined ground squirrel. Biochim Biophys Acta, 1850 2196-202. https:// doi.org/10.1016/j.bbagen.2015.07.004

Wu, W.F., Maneix, L., Insunza, J., Nalvarte, I., Antonson, P., Kere, J., Yu, N.Y., Tohonen, V., Katayama, S., Einarsdottir, E., Krjutskov, K., Dai, Y.B., Huang, B., Su, W., Warner, M. & Gustafsson, J. (2017) Estrogen receptor β, a regulator of androgen receptor signaling in the mouse ventral prostate. Proc Natl Acad Sci U S A. 114(19), E3816-E3822. https://doi:10.1073/pnas.1702211114

Xi, M. & Tang, W. (2020) Knockdown of Ezrin inhibited migration and invasion of cervical cancer cells in vitro. Int J Immunopathol Pharmacol. 34, 2058738420930899. https://doi:10.1177/2058738420930899

Yang, H.P., Meeker, A., Guido, R., Gunter, M.J., Huang, G.S., Luhn, P., d'Ambrosio, L., Wentzensen, N. & Sherman, M.E. (2015) PTEN expression in benign human endometrial tissue and cancer in relation to endometrial cancer risk factors. Cancer Causes Control. 26(12), 1729-1736. https://doi:10.1007/s10552-015-0666-5

Yu, H.F., Chen, H.S., Rao, D.P. & Gong, J. (2016) Association between polycystic ovary syndrome and the risk of pregnancy complications: A PRISMA-compliant systematic review and meta-analysis. Medicine (Baltimore). 95(51), e4863. https://doi:10.1097/md.0000000000004863

Zhang, Y., Hu, M., Meng, F., Sun, X., Xu, H., Zhang, J., Cui, P., Morina, N., Li, X., Li, W., Wu, X.K., Brännström, M., Shao, R. & Billig, H. (2017) Metformin Ameliorates Uterine Defects in a Rat Model of Polycystic Ovary Syndrome. EBioMedicine. 18, 157-170. https://doi:10.1016/j.ebiom.2017.03.023

Zhao, P.L., Zhang, Q.F., Yan, L.Y., Huang, S., Chen, Y. & Qiao, J. (2014) Functional investigation on aromatase in endometrial hyperplasia in polycystic ovary syndrome cases. Asian Pac J Cancer Prev. 15(20), 8975-8979. https://doi:10.7314/apjcp.2014.15.20.8975

Zheng S., Chen Y., Ma M. & Li M. (2022) Mechanism of quercetin on the improvement of ovulation disorder and regulation of ovarian CNP/NPR2 in PCOS model rats. J Formos Med Assoc, 121 1081-1092. https:// doi:10.1016/j.jfma.2021.08.015

Zukerberg, L.R., DeBernardo, R.L., Kirley, S.D., D'Apuzzo, M., Lynch, M.P., Littell, R.D., Duska, L.R., Boring, L. & Rueda, B.R. (2004) Loss of cables, a cyclin-dependent kinase regulatory protein, is associated with the development of endometrial hyperplasia and endometrial cancer. Cancer Res. 64(1), 202-208. https://doi:10.1158/0008-5472.can-03-2833

892 **Table 1.** Primers and PCR products for real time quantitative PCR

Gene	Accession Number	Primer Sequences	Size (bp)	Ta (ºC)
Star	NM_031558.3	F: 5' GCAAAGCGGTGTCATCAG '3 R: 5' GGCGAACTCTATCTGGGTCT '3	172	57
Akr1c14	NM_138547.3	F: 5' GCACTCAACTGGACTATGTGGA '3 R: 5' GCTCATCTCGTGGGAAAAAT '3	87	50.7
Hsd3b1-3,5	NM_001007719.3, NM_017265.4, NM_001042619.1 NM_012584.1	F: 5´ CCTGGATGGAGCTGCCTG ´3 R: 5´ CCTGGCACGCTCTCCTCA ´3	220	61
Hsd3b7	NM_139329.1	F: 5´ GAGCGGAAGGAAGGAAGCCT ´3 R: 5´ AGGAAGCCACAGCCACCTGT ´3	167	61
Hsd17b1	NM_012851.2	F: 5´ AGATACTGGAATTGGATGTCA ´3 R: 5´ AAGAACATTCACATCCAGTACA ´3	170	56
Hsd17b2	NM_024391.1	F: 5´ AGCGGAGGAATTGAGGAA ´3 R: 5´ AGACCCCAGCATTGTTGA ´3	152	56
Hsd17b3	NM_054007.1	F: 5' AGTACCTAAATACCAGCAGGG '3 R: 5' GGTGCTGCTGTAGAAGATTCT '3	161	55
Hsd17b4	NM_024392.2	F: 5´ GACAGCACTGGACACATTCG ´3 R: 5´ TATGATCCCATGCTGCCC ´3	161	57
Srd5a1	NM__017070.3	F: 5' CACCTTCAACGGCTATGTAC '3 R: 5' AGGATGTGGTCTGAGTGGAT '3	144	54
Srd5a2	NM_022711.4	F: 5' TTGTGGTGTCGGTAGGGATG '3 R: 5'CAGAAGGCAGTGGCTCTCAA'3	175	56
Cyp2d4	NM_138515.2	F: 5' CGCTGGACTTCTCGCTA '3 R: 5' CGGTGTCCTCGCTGTAT '3	214	57
Cyp17a1	NM_012753.2	F: 5'GGTGATAAAGGGTTATGCCA '3 R: 5'GCTTGAATCAGAATGTCCGT '3	117	55
Cyp19a1	NM_017085.2	F: 5' TGGCAGATTCTTGTGGATGG ´3 R: 5' CGAGGACTTGCTGATGATGAGT ´3	118	54
Sts	NM_012661.1	F: 5' CTTGAGGGGGTGAAGTTGAC '3 R: 5' CCCAGATGATGCCGAGAA '3	150	58

Esr1	NM_012689.1	F: 5'- ACTACCTGGAGAACGAGCCC -3' R: 5'- CCTTGGCAGACTCCATGATC -3'	153	60
Esr2	NM_012754.3	F: 5'- TTCTGGGCACCTGTCTCCTT -3' R: 5'- TAACAGGGCTGGCACAACTG-3'	167	57
Ar	NM_012502.1	F: 5'- AGGGAGGTTACGCCAAAG -3' R: 5'- AGACAGTGAGGACGGGAT -3'	101	58
Pten	NM_031606.2	F: 5´ TTATTGCTATGGGATTTCCT 3´ R: 5´ GGTTTTTATGCTTTGAATCC 3´	96	53
Wnt5a	NM_022631.3	F: 5'-CCTGTAGCCTCAAGACATGCTGG-3 R: 5'-GAGTTGAAGCGGCTGTTGACCT -3	142	60
Wnt7a	NM_001100473.1	F: 5'-CTTACACAATAACGAGGCAGGC-3 R: 5'-TCTCGGAATTGTGGCAGTGT-3'	126	56
Hoxa10	NM_018951.4	F: 5'-GAAAACAGTAAAGCCTCTCC-3' R: 5'-ATAGAAACTCCTTCTCCAGC-3'	148	54
Ctnnb1	NM_053357.2	F: 5'-GAGCACATCAGGACACCCAGC-3' R: 5'-GAGGATGTGGAGAGCCCCAGT-3'	116	60
Rpl19	NM_031103.1	F: 5'-AGCCTGTGACTGTCCATTCC-3' R: 5'-TGGCAGTACCCTTCCTCTTC-3'	99	60

F: forward, R: reverse, Ta: annealing temperature

Table 2. Epithelial and glandular abnormalities observed in the uterine tissue of PCOS and PCOS-F rats

	CONTROL	PCOS	PCOS-F
EPITHELIAL ABNORMALITIES #	**28.6% [a]**	**100% [b]**	**87.5% [b]**
Hyperplasia of the luminal epithelium*	0/7 (0%) [a]	8/11 (72.7%) [b]	5/8 (62.5%) [b]
Intraepithelial lumens*	0/7 (0 %) [a]	8/11 (72.7%) [b]	7/8 (87.5%) [b]
Intraepithelial glandular formation*	2/7 (28.6%) [a]	10/11 (90.9%) [b]	7/8 (87.5%) [b]
Polyps*	0/7 (0%) [a]	8/11 (72.7%) [b]	5/8 (62.5%) [b]
Luminal epithelial height	22 ± 2 µm [a]	44 ± 5 µm [b]	38 ± 4 µm [b]
GLANDULAR ABNORMALITIES #	**0% [a]**	**81.8% [b]**	**100% [b]**
Cystic glands*	0/7 (0%) [a]	5/11 (45.5%) [ab]	5/8 (62.5%) [b]
Conglomerates of glands*	0/7 (0%)	5/11 (45.5%)	4/8 (50%)
Glands with metaplasia*	0/7 (0%)	2/11 (18.2%)	3/8 (37.5%)
Glands with cellular atypia*	0/7 (0%) [a]	6/11 (54.5%) [b]	8/8 (100%) [b]
Glandular density	0.019 ± 0.002 [a]	0.028 ± 0.001 [b]	0.033 ± 0.003 [b]

Percentage of rats with at least one abnormality.
* The incidence of abnormalities is expressed as percentage of females with a specific lesion.
Different letters indicate significant differences between groups ($p < 0.05$).

916 **Table 3**. Uterine endocrine status

	CONTROL	PCOS	PCOS-F
STEROID SERUM LEVELS			
Testosterone (ng/mL)	Not detected	0.55 ± 0.09	0.46 ± 0.03
17β-estradiol (pg/mL)	65.2 ± 3.9	55.8 ± 4.1	55.5 ± 2.6
Progesterone (ng/mL)	9.7 ± 2.7	7.4 ± 2.5	4.5 ± 2.8
UTERINE STEROIDS			
Testosterone	66.7%	Not detected	66.7%
17β-estradiol	100%	100%	100%
Estrone	100%	75%	66.7%
Progesterone	100%	50%	100%
STEROID RECEPTORS EXPRESSION			
mRNA expression			
Esr1	1.07 ± 0.09 **a**	0.92 ± 0.08 **a**	0.86 ± 0.09 **a**
Esr2	0.003 ± 0.0006 a	0.0009 ± 0.0002 b	0.0007 ± 0.00007 **b**
Ar	0.46 ± 0.03 **a**	0.77 ± 0.06 **b**	0.56 ± 0.02 **a**
Protein expression			
ESR1 (subepithelial stroma)	2.02 ± 0.64 **a**	1.43 ± 0.29 **a**	0.47 ± 0.09 **b**
ESR1 (myometrium)	0.65 ± 0.19 **ab**	0.90 ± 0.18 **a**	0.32 ± 0.07 **b**
ESR2 (subepithelial stroma)	1.02 ± 0.15 **a**	0.57 ± 0.03 **b**	0.61 ± 0.04 **b**
ESR2 (myometrium)	0.40 ± 0.04 **a**	0.23 ± 0.04 **b**	0.16 ± 0.01 **b**
AR (subepithelial stroma)	1.37 ± 0.17 **a**	2.09 ± 0.27 **b**	1.02 ± 0.12 **a**
AR (myometrium)	0.63 ± 0.09 **a**	1.25 ± 0.12 **b**	0.88 ± 0.17 **ab**

917

918 Steroid serum levels are expressed as mean ± SEM.
919 Uterine steroids are expressed as percentage of rats with detected levels of each hormone.

Esr1, Esr2 and *Ar* mRNA were expressed as relative units. The samples were normalized to *Rpl19* mRNA as a housekeeping gene.
ESR1, ESR2 and AR protein were evaluated as integrated optical density (arbitrary units).
Different letters indicate statistically significant differences between groups ($p<0.05$).

Highlights

- PCOS increases the incidence of uterine epithelial and glandular lesions.
- PCOS induces uterine steroid metabolism alterations.
- In the uterus, AR and aromatase expression are AR-dependent and an ESR2-ESR1-AR crosstalk is suggested.
- In PCOS rats, altered PTEN and WNT5a expression is associated with uterine differentiation changes.

DECLARATION OF CONFLICTING INTERESTS

The authors declare that there are no conflicts of interest that could be perceived as prejudicing the impartiality of the research reported.